

Putting a bug in ML: The moth olfactory network learns to read MNIST

Charles B. Delahunt* and J. Nathan Kutz†

Abstract. We seek to (i) characterize the learning architectures exploited in biological neural networks for training on very few samples, and (ii) port these algorithmic structures to a machine learning context. The *Moth Olfactory Network* is among the simplest biological neural systems that can learn, and its architecture includes key structural elements widespread in biological neural nets, such as cascaded networks, competitive inhibition, high intrinsic noise, sparsity, reward mechanisms, and Hebbian plasticity. The interactions of these structural elements play a critical enabling role in rapid learning.

We assign a computational model of the Moth Olfactory Network the task of learning to read the MNIST digits. This model, MothNet, is closely aligned with the moth’s known biophysics and with *in vivo* electrode data, including data collected from moths learning new odors. We show that MothNet successfully learns to read given very few training samples (1 to 20 samples per class). In this few-samples regime, it substantially outperforms standard machine learning methods such as nearest-neighbors, support-vector machines, and convolutional neural networks (CNNs). The MothNet architecture illustrates how our proposed algorithmic structures, derived from biological brains, can be used to build alternative deep neural nets (DNNs) that may potentially avoid some of DNNs current learning rate limitations. This novel, bio-inspired neural network architecture offers a valuable complementary approach to DNN design.

1. Introduction.

Originally inspired by the biological structure of networks of interacting neurons [1, 2], neural networks (NNs) have since developed a suite of algorithmic tools (such as backprop, convolutional kernels, etc) which, combined into complex and deep NN architectures, have achieved unprecedented success in a wide array of machine learning (ML) tasks [3, 4, 5]. However, they are also known to fail on critical tasks such as learning from few samples. We seek to improve NN performance on such tasks by revisiting the well of biological example to characterize key biological structures involved in learning, for transfer to the DNN context. Specifically, we develop a NN architecture based on the moth olfactory system that successfully learns to read given very few training samples (1 to 20 samples per class) and that outperforms standard machine learning methods, such as nearest-neighbors, support-vector machines, and convolutional neural networks (CNNs), in the few-sample regime (Fig 4.1).

The Moth Olfactory Network is among the simplest biological neural networks (BNNs) that can learn [6]. It is well-characterized, and it contains key features widespread in BNNs, including high noise [7], random connections [8], Hebbian synaptic growth [9, 10], high-dimensional sparse layers [11, 12], large dimension shifts between layers [13], and generalized stimulation of neurons during learning [14, 15]. It thus offers an ideal avenue to investigate biological learning and the interacting components that make learning possible.

The olfactory processing unit centers on two interacting networks, the noisy antennal lobe (AL) and the sparse mushroom body (MB), known as the AL-MB [16, 11]. The AL acts as a pre-processor, and projects the odor signal forward to the MB. Learning occurs when

*Department of Electrical Engineering, University of Washington, Seattle, WA, USA. delahunt@uw.edu

†Department of Applied Mathematics, University of Washington, Seattle, WA, USA. kutz@uw.edu

a reward mechanism (sucrose) induces an overall increase in excitation in the AL via the neuromodulatory chemical octopamine [17]. This induces Hebbian updates to plastic synaptic weights in the plastic MB, i.e. modulating one network rewires another. Sparsity in the MB controls Hebbian plasticity by filtering noise and focusing training gains on relevant signals. In combination, these features enable rapid and effective learning, expressed as permanent modulation of readout neuron responses to trained odors [18].

MothNet is an end-to-end computational model of the *Manduca sexta* (Hawk moth) olfactory network that is closely based on its known biophysical structure, is consistent with *in vivo* firing rate data, and incorporates learning behavior [18]. We assigned MothNet the classic ML task of identifying the handwritten digits of the MNIST dataset [19]. MothNet routinely achieved 75% to 85% accuracy classifying test digits after training on 1 to 20 samples per class, out-performing standard ML methods. The results demonstrate that even a very simple biological architecture contains novel and effective tools applicable to ML tasks, in particular tasks constrained by few training samples or the need to add and train new classes without retraining the full NN.

2. The moth olfactory network and MothNet model.

2.1. Moth olfactory network.

A brief outline of the moth olfactory network architecture is given here. For more detail see [18]. The network is organized as a feed-forward cascade of five distinct networks, as well as a reward mechanism [20, 21]. Fig 2.1 gives a system schematic.

Starting at the Antennae, several thousand noisy chemical Receptor Neurons (RNs) detect odor and send signals to the Antennal Lobe (AL) [16, 10]. The AL acts as a pre-amp, providing gain control and sharpening odor codes through lateral inhibition [22]. The AL contains roughly 60 isolated units (glomeruli), each focused on a single odor feature [20]. The AL projects odor codes forward to the Mushroom Body (MB) [11], in excitatory Projection Neurons (PNs) that randomly connect to MB neurons [8].

The MB contains about 4000 Kenyon Cells, which fire sparsely and encode odor signatures as memories [23, 12] (we use “MB” as a synonym for these Kenyon Cells). Sparsity in the MB is enforced by global inhibition from the Lateral Horn [24]. The MB feeds forward to Extrinsic Neurons (ENs), numbering ~ 10 ’s, which are “readout neurons” that interpret the MB codes and deliver actionable output to the rest of the moth [25, 26].

The network can learn: In response to reward (sugar at the proboscis), a large neuron sprays the neuromodulator octopamine globally over the AL and MB. Octopamine stimulates AL neurons, inciting higher firing rate responses to the reinforced stimuli, which in turn induce growth in the plastic synaptic connections into the MB (AL \rightarrow MB) and out of the MB (MB \rightarrow ENs) [9, 10]. Learning does not occur without this octopamine input [14, 15].

2.2. MothNet model.

The MothNet computational model closely follows this architecture in terms of connections, numbers of neurons in each layer, etc [18]. Neural firing rates are modeled with integrate-and-fire dynamics [27] evolved as stochastic differential equations (SDEs) [28]:

$$(2.1) \quad \tau \frac{dx}{dt} = -x + s(\Sigma \mathbf{w}_i \mathbf{u}_i) = -x + S(\mathbf{w} \cdot \mathbf{u}) + dW,$$

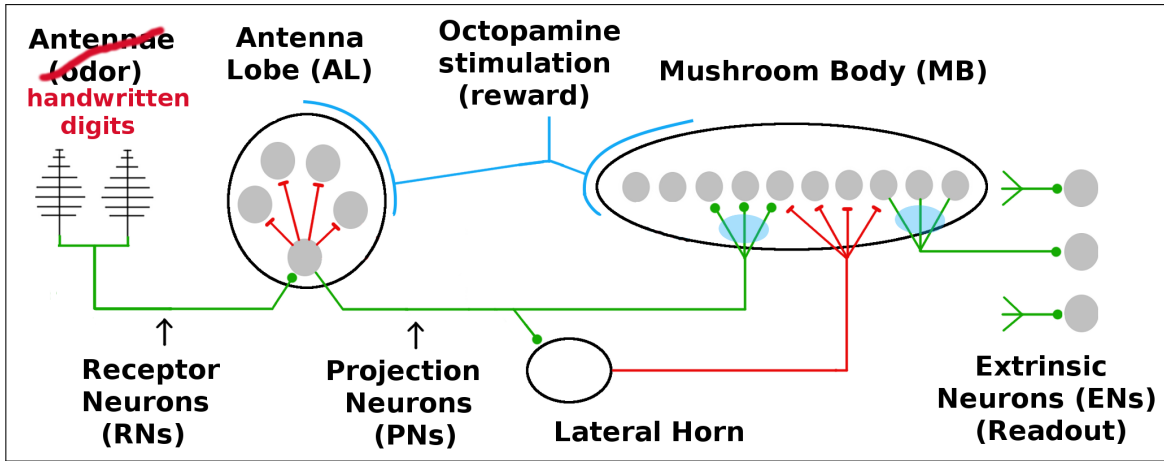


Figure 2.1. Network schematic. Green lines show excitatory connections, red lines show inhibitory connections. Light blue ovals show plastic connections into and out of the MB. The glomeruli (processing units) in the AL competitively inhibit each other. Global inhibition from the lateral horn induces sparsity on MB responses. The ENs give the final, actionable readouts of the system’s response to a stimulus.

where $x(t)$ = firing rate (FR) for a neuron, \mathbf{w} = connection weights, \mathbf{u} = upstream neuron FRs, $S()$ is a sigmoid function or similar, and $W(t)$ = a brownian motion process.

The model uses Hebbian plasticity for synaptic weight updates [29, 27]:

$$(2.2) \quad \Delta w_{ab}(t) = \gamma f_a(t) f_b(t)$$

where $f_a(t), f_b(t)$ are firing rates of neurons a, b at time t , w_{ab} is the synaptic weight between them, and γ is a growth rate parameter.

In addition, inactive MB→EN weights are subject to proportional decay:

$$(2.3) \quad \Delta w_{ab}(t) = \delta w_{ab}(t), \text{ if } f_a(t) f_b(t) = 0.$$

where δ is a decay parameter. There are two layers of plastic synaptic weights: AL→MB, and MB→ENs (ie pre- and post-MB). Hebbian plasticity is assumed to be “switched on” by reward, so it is cosynchronous with octopamine. Thus, plasticity only occurs during training sessions.

For the MNIST task, MothNet has 10 extrinsic neurons (ENs), that start with identical MB→EN connections. When training begins, these 10 ENs are randomly assigned to target particular digits 0 to 9. Once ENs are assigned, training is supervised: When a digit of class j is presented, only MB→EN $_j$ connections are updated, where EN $_j$ is the EN assigned to class j . That is, the system knows the class of the training sample, for the purposes of post-MB updates. Training rapidly individualizes these weights according to their target digits. In contrast, all pre-MB connections are updated in every case, since these connections are common to all inputs (these updates are slower).

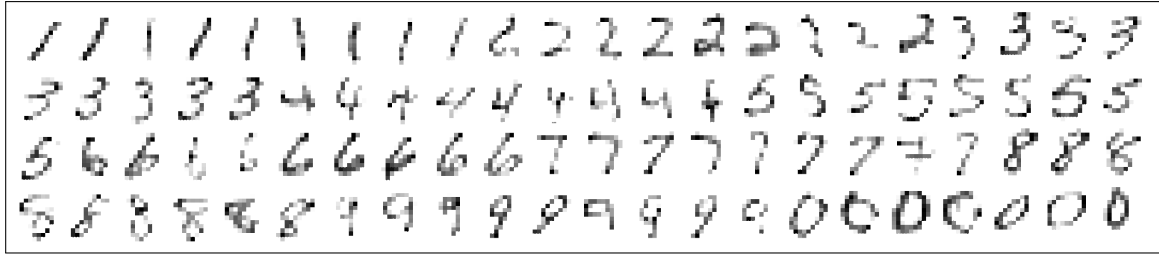


Figure 3.1. Downsampled MNIST digits used in the experiments (random selection).

3. Methods.

3.1. Training data.

The MNIST dataset consists of grey-scale thumbnails, 28×28 pixels, of handwritten digits 0 to 9. We used the MNIST dataset package in PMTK3 [30]. We used pixels of the thumbnails as input features to the MothNet classifier. Both biological and engineered systems routinely choose better feature sets. However, pixels-as-features provide a good test of whether MothNet can effectively learn to discriminate classes given inputs with inter-class correlations.

MothNet (like the moth) feeds one feature to each glomerulus in the AL. Using full MNIST thumbnails, with pixels-as-features, would imply $28^2 = 784$ glomeruli. To keep the scale of MothNet somewhat close to that of the true moth (60 glomeruli), we preprocessed the thumbnails as follows:

1. Downsample by 2 (linear interpolation).
2. Mean-subtract using 500 random, set-aside digits (50 from each class).
3. Select only the most-active pixels by thresholding the various class averages, ie retain only the most generally active pixels in the thumbnails while also preserving the most active pixels of each class. These pixels define the receptive field, and exclude border pixels which supply no information.

Each retained pixel became a feature that fed into one glomerulus of MothNet's AL. The experiments described here used 83 pixels (out of $14^2 = 196$ total) to represent the MNIST digits. Examples of digit thumbnails are shown in Fig 3.1.

3.2. Experiment design.

Moth generation. Particular MothNet behaviors can be modulated by varying one or two template parameters. Each experiment used a fixed basic moth template, modified only by varying the parameter(s)-under-test. Each of these modified templates then randomly generated many moths, typically 13-17 per data point. The basic templates varied slightly between experiments, eg in some parameter values. We found that these slight differences in moth template had minor effect, and that a wide range of parameters and templates delivered effective learning behavior.

Experiment sequence of events. Each experiment contained three stages:

1. Pre-training Baseline (15 digits per class), used to assess naive classifier accuracy;

2. Training (equal numbers of digits per class, randomly ordered);
3. Post-Training Validation (15 digits per class), used to assess post-training classifier accuracy.

Digits for each stage were randomly chosen without replacement from non-intersecting pools. Using more than 15 digits in baseline and validation sets did not significantly affect results.

Since the moth olfactory system can learn to recognize a new odor given roughly 8-10 samples [6], we focused on small training sets (1-20 samples/class). In some experiments, training included multiple “sniffs”, ie repeated presentations of each sample. The order of training samples did not matter, perhaps because the strongest plasticity was specific to the readout neuron (EN) targeting a given class and was focused on the active pixels of that class.

3.3. Classifiers.

System readout units are the Extrinsic Neurons (ENs) downstream from the sparse MB layer and its plastic connections. These ENs are silent absent any input sample, and they consistently respond, more or less strongly, to input samples (see Fig 4.2). We classified test digits using a summed log-likelihood over the distributions of responses to each digit class in each EN:

$$(3.1) \quad \hat{s} = \min_{j \in J} \left\{ \sum_{i \in J} \left(\frac{E_i(s) - \mu E_{ij}}{\sigma E_{ij}} \right)^4 \right\}, \text{ where}$$

\hat{s} = predicted class of sample s

$E_i(s)$ = response of the i th EN to s

μE_{ij} = mean($E_i(t) | t \in V, t \in \text{class } j$)

σE_{ij} = std dev($E_i(t) | t \in V, t \in \text{class } j$)

$j \in J$ are the classes (0-9)

V is a reference set (eg a validation set).

Roughly, j is a strong candidate for \hat{s} if each EN’s response to s is close to that EN’s expected response to class j . The use of the 4th power (vs the usual 2nd power) is a sharpener that penalizes outliers.

This summed log-likelihood is a measure of how well the ENs can separate the response distributions to various classes, combining information from all ENs and including information about responses to classes not specifically targeted by a particular EN. The goal of this classifier is to assess how much discriminatory information MothNet was able to extract from the training data. We do not wish to imply it is biologically realistic (we don’t know). Accuracy of naive (ie untrained) moths was about 15%, slightly higher than random guessing, perhaps because the digit “1” often elicited slightly different naive responses than other digits.

For a given experiment, the post-training classification accuracy was calculated on the validation set, ie the same set used to estimate the post-training EN response distribution parameters μE and σE . Similarly, the baseline (pre-training) classification accuracy was calculated on the same baseline set used to estimate naive EN response distribution parameters. We used the validation set to assess post-training discrimination (rather than a separate holdout set) to shorten simulation time, and also because this was sufficient for the purpose

of assessing the increase in discrimination from baseline. Results for true holdout sets were roughly the same.

A more biologically plausible classifier might be simple thresholding: Label the test sample as the class of the most responsive EN_j (by Mahalanobis distance),

$$(3.2) \quad \hat{s} = \max_{j \in J} \left\{ \frac{E_j(s) - \mu E_{jj}}{\sigma E_{jj}} \right\}, \text{ notation as in Eqn. (3.1).}$$

This uses no cross-class information (E_i response to $s \in$ class $i \neq j$).

Accuracy of classification by simple thresholding was in general much lower than by the log-likelihood classifier, likely because thresholding does not leverage the full information about each EN's responses to every class, but only each EN_j 's response to its assigned class j . For general ML applications, biological plausibility of the classifier is not required.

4. Experiments and Results.

This section presents (i) a baseline comparison to standard ML methods, then gives results of MothNet experiments focused on (ii) Learning, (iii) one-shot learning, (iv) sniffing, and (v) effects of AL noise, and (vi) MB sparsity.

4.1. Comparison to standard ML methods.

To set a learning performance baseline, we trained three standard ML methods (Nearest Neighbors, SVM, and CNN) in the few-training-samples regime (1 to 20 training samples per class), using the same sample pre-processing (except CNN, see below). We note that while these ML methods can attain over 99% accuracy on the full MNIST training set (6000 samples per class) [31], the few-samples regime is fundamentally different, and standard ML methods are evidently not well suited to it, compared to biological systems. This few-samples regime can be roughly visualized, for MNIST, as follows: First throw away 99.9% of the usual training data; then begin training.

In this few-samples regime, MothNet substantially out-performed the three ML methods. Mean post-training accuracies of the various methods are plotted in Fig 4.1, vs number of training samples per class. Given ≤ 5 training samples, MothNet had roughly double the accuracy of ML methods (eg 60 - 70% vs 30 - 35%, on 3 samples). For equivalent accuracy levels, ML methods required between 2x and 10x more training data than the “natural moth”, and between 20x to 50x more training data than the “fast moth”.

The MothNet accuracies shown in Fig 4.1 are the same as those given in Fig 4.4A. The “natural moth” was a version of MothNet closest to those tuned to match *in vivo* electrode data and natural learning behavior in [18]. The “fast moth” was a version of MothNet with artificially high learning rate parameters. Nearest-Neighbors used Matlab’s “fitcknn” function with standardized variables, and with number-of-neighbors optimized for each number-of-training-samples case. SVM used Matlab’s “fitcecoc” function with standardized variables, and with box constraint optimized for each number-of-training-samples case. The CNN was that of Matlab’s example “nnet/TrainABasicConvolutionalNeuralNetworkForClassificationExample”, with the number of epochs optimized for each number-of-training-samples case. The features for Nearest-neighbors and SVM were pixels from thumbnails pre-processed just as for MothNet. The CNN used the standard MNIST (28x28) thumbnails, on which it can readily attain

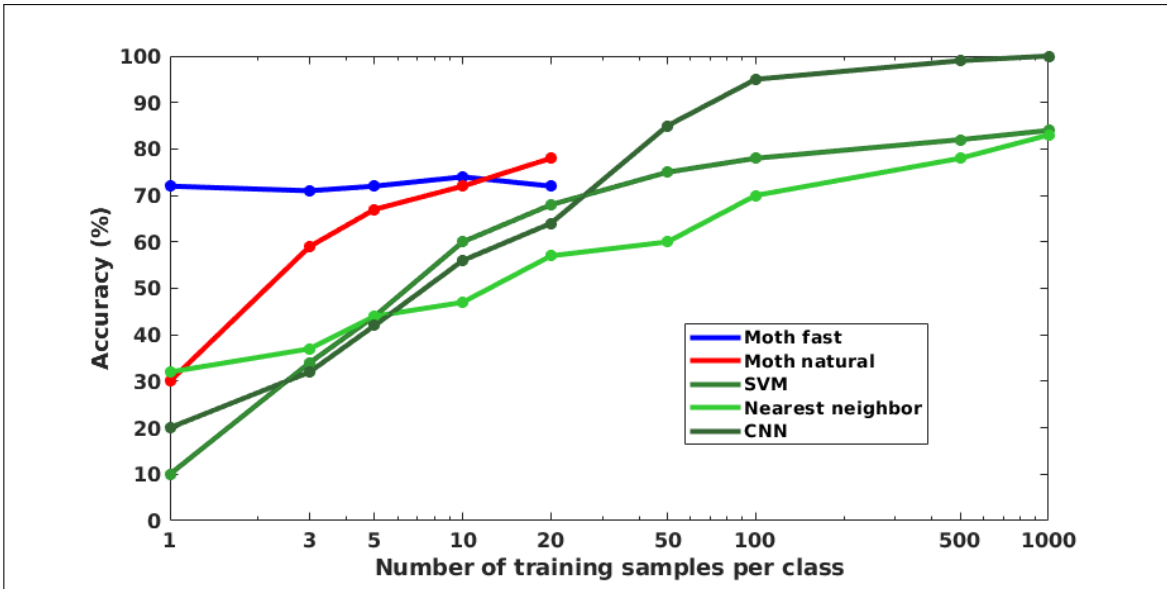


Figure 4.1. Mean post-training accuracy for fast- and natural-learning MothNet moths, as well as for Nearest-neighbors, SVM, and CNN, vs log of training samples per class. In the few-training-samples regime (1 to 20 per class), MothNet substantially outperformed standard ML methods.

> 99% accuracy given sufficient training data. This obviated the need to alter the CNN network parameters to fit smaller images, and thus guaranteed a capable architecture.

4.2. Learning experiments.

We ran training experiments with various moth templates to assess their ability to learn the MNIST digits. In general, a wide range of moth templates responded well to training by differentiating their EN responses to different digits (input classes). In naive moths, all ENs had the same response profile, and responded similarly to all digit classes, as expected given the symmetry of random connection strengths to MB and to the various ENs. Training caused EN responses to diverge from baseline and from each other, such that each EN responded most strongly to its assigned digit. Common effects of training included:

1. Most ENs (eg 1, 2, 6, 7, 0) tended to amplify the response to their trained digit very well, compared to responses to control digits. This gave strong separation and accurate classification.
2. A few ENs (eg 5) sometimes poorly separated their trained digit from control digits. These were the digits most often misclassified during validation.
3. Some ENs consistently boosted the responses to certain control digits along with their trained digit (eg, EN₉ boosted 4 and 7, EN₄ boosted 7 and 9). These cases typically reflected visible similarities in the digits, and led to characteristic errors. For example, 9s, if misclassified, were often misclassified as 4s. However, 9's were not misclassified as 7s, because EN₇ usually strongly separated 7 from 9. That is, outputs of EN₉, EN₇, and EN₄ combined were sufficient to distinguish 9 from 7, but not always 9 from 4.

These behaviors are evident in Fig 4.2, which shows timecourses of EN firing rate responses,

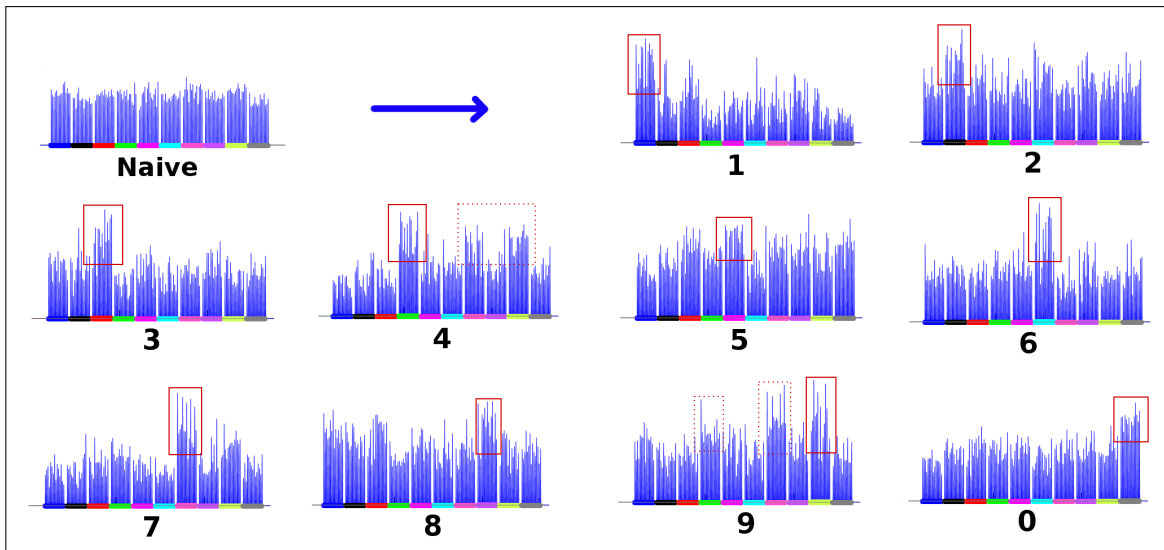


Figure 4.2. Pre- and post-training EN time courses (normalized) for a typical moth trained on 15 samples per class, showing post-training separation. Each timecourse shows EN response to 150 digits (15 ones, then 15 two's, etc). Top left = naive response (all ENs similar). Other subplots show trained ENs (trained class responses framed in red, some confounding class responses in dashed red).

pre- and post-training, for a typical moth. Each subplot shows EN response to 150 digits (15 ones, then 15 two's, etc). The post-training responses are normalized by the EN's mean trained class response for clarity. Training typically increased and/or decreased all class responses of an EN, but to different degrees, resulting in the separations seen in the normalized timecourses. Training stage responses are excised from the timecourses to save space; these responses were consistently much stronger due to the stimulating effect of octopamine injected during training, and would extend past the top of the plot.

Fig 4.3 plots EN response distribution statistics (mean \pm std dev) from a typical experiment, in which 13 moths were generated from a template, then trained on 15 samples per class. Post-training accuracy for moths of this template was 71-83%, starting from \sim 15% baseline accuracy. Similar results, both accuracies and limitations (such as confusing 4s and 9s) held for a wide range of moth templates and training regimes. These learning experiments indicate that the moth olfactory network, with minimal modifications, can rapidly learn to read handwritten digits.

4.3. Growth rate effects, one-shot learning.

The speed at which MothNet learns, ie the number of training samples required to reach maximum accuracy, is determined to large degree by the Hebbian growth rate on MB \rightarrow EN connections and the related decay rate on MB \rightarrow EN connections. When the connection weights hit the rails of their dynamic range, no further learning is possible (we did not modify the maximum synaptic weight constraints). We ran experiments to study the effect of Hebbian growth rates on post-training accuracy, given various training set sizes. One moth template (the “natural learner”) had a biologically plausible growth rate (per *in vivo* data), while the second moth template (the “fast learner”) had a growth rate “turned up to 11”. High growth

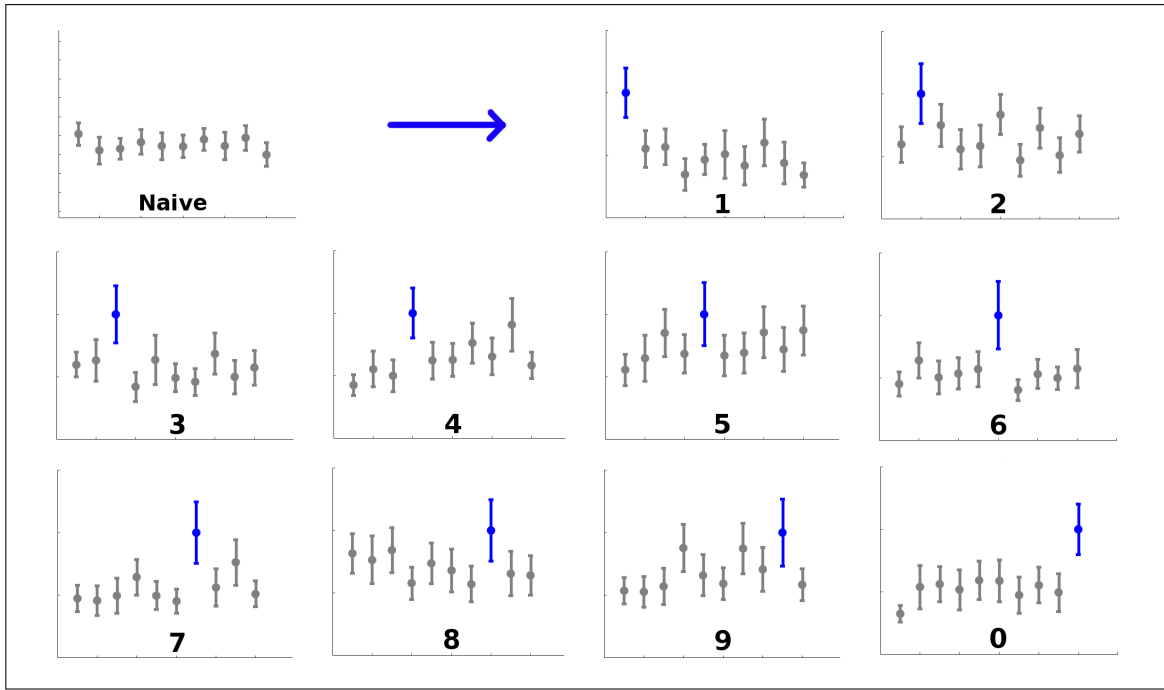


Figure 4.3. Pre- and post-training EN response distributions (normalized) from a typical experiment, showing post-training separation of class response distributions. Dots show $\text{mean}(\mu)$, bars show $\text{mean}(\sigma)$ averaged over μ and σ from 13 moths. Mean accuracy for this template was 76%, range 71-83%. Top left = naive response (all ENs similar). Other subplots show trained EN responses in blue. 10 training samples/class.

rate moths allowed us to test MothNet’s skill at one-shot learning (ie given just one training sample).

Fast learners attained strong immediate accuracy (mean 75%) on just one training sample, but additional training samples provided no further gain. Natural learners took several (~ 20) training samples to attain maximum accuracy, but that final accuracy was higher ($\sim 80\%$). When classification was done by simple thresholding (Eqn 3.2) rather than the log-likelihood method (Eqn 3.1), the long-term advantage of natural over fast learners was more pronounced (43% vs 33%). The trade-off of learning speed vs maximum attained accuracy is seen in Fig 4.4A. The solid curves show fast- and natural-learner accuracies vs number of training samples. The dashed curves show results from the same experiments, using simple thresholding as an alternative classifier. The effect is similar, but the short-term/long-term contrast is stronger.

Fig 4.4A incidentally shows the lower accuracy delivered by using thresholds on EN responses (Eqn 3.2 rather than the log-likelihood classifier Eqn 3.1). The difference seen here (80% vs 40%) was typical.

4.4. Sniffing, effects of AL noise.

Sniffs. Biological NNs have a remarkable ability to learn from very few training samples. In addition, “sniffing” behavior (repeated sampling of a given odor) is a common biological strategy [16, 20]. We ran experiments to see whether sniffing behavior improved the various

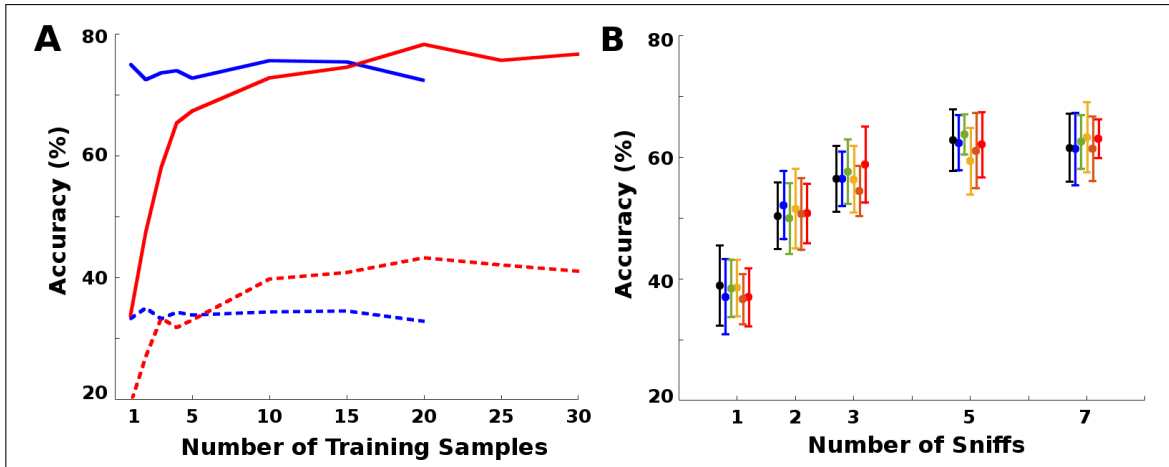


Figure 4.4. **A:** Effects of growth rate. Solid horizontal blue curve = very fast learner. Solid ascending red curve = natural learner. The fast learner attained 75% accuracy in one-shot, but with no further gains. The natural learner ultimately attained higher accuracy. Dotted lines show the same effect in accuracy using threshold classifier. **B:** Effects of sniffing and noise on one-shot learning, in a “natural-learner” moth template. Multiple sniffs greatly improved one-shot accuracy. Noise in the AL: The clusters of $\mu \pm \sigma$ bars represent varying levels of AL noise, with low-to-high noise plotted left-to-right at each x-axis location. AL noise level did not affect accuracy. 13 moths per data point.

stages of learning. Sniffing applied to test samples did not improve test accuracy (experiments not shown).

However, sniffing during training had a large effect, especially in one-shot regimes. When a “natural learner” (ie the template’s learning rate was set to a biologically reasonable level) was given a single training sample (one-shot), multiple sniffs raised post-training accuracy from 35% to over 60%. Five sniffs delivered maximal increase, with no further gains from additional sniffs. This increase in accuracy due to sniffing in the one-shot context is seen in Fig 4.4B. Multiple sniffs (up to 5) during training dramatically improved accuracy. More than 5 sniffs yielded no further benefit.

AL noise. The moth AL is a very noisy system. That is, neural responses to a given odor stimulus (or absent any odor) have high variance. To see whether this AL noise was beneficial to learning performance, we also varied the AL noise level during the above sniffing experiments, from near-zero through the high end of biologically reasonable (per wet lab data). We had expected the presence of AL noise to improve performance, given multiple sniffs, by acting as a kind of sample augmentation, analogous to that used in DNN training. In fact, noise levels in the AL had no effect on accuracy. This is seen in Figure 4.4B, where each cluster of mean \pm std dev bars shows different levels of AL noise for a given number of sniffs.

4.5. Sparsity experiments.

High-dimensional, sparse neural layers are a widespread motif in biological NNs [32]. To examine the effects of sparsity in the context of learning the MNIST digits, we trained a reasonably capable moth template, varying only the sparsity level in the MB during training (17 moths per sparsity level). Sparsity here is measured as the fraction of MB neurons that are responsive to stimuli (1% is very sparse, 50% is very dense). In MothNet, MB sparsity

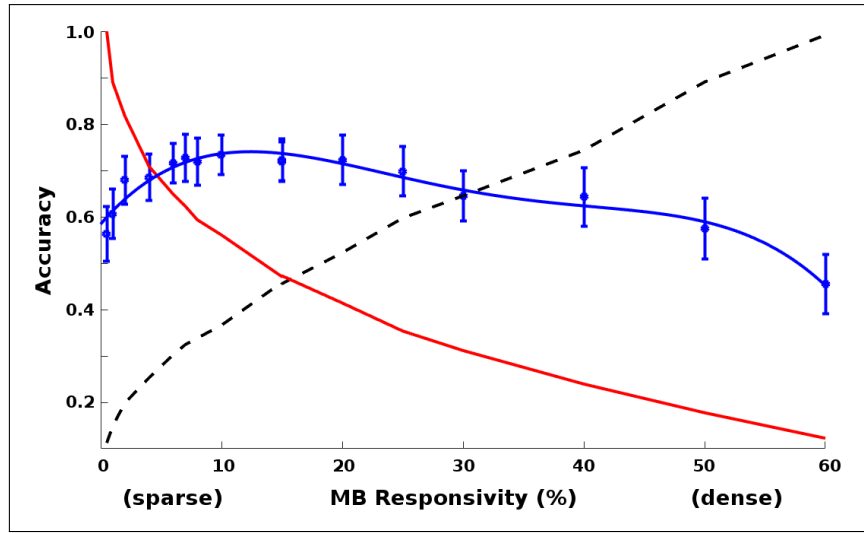


Figure 4.5. Effects of sparsity in the MB: Optimal accuracy (blue domed curve, $\mu \pm \sigma$) occurred at 5-20%, a compromise between learning focus and high intra-class signal-to-noise ratio (SNR). Descending red curve = mean separation of trained vs control (learning focus). Black ascending curve = mean intra-class SNR. Learning focus and SNR are scaled for plotting. 17 moths per sparsity level.

levels (in both non-training and training modes) are parameters. Sparsity levels in the MB affected two crucial behaviors: Intra-class signal-to-noise ratio (SNR) of EN responses; and how well a given EN_j 's response to training focused on class j .

Results showed that the sparse MB layer plays a key role in learning by controlling and focusing Hebbian weight updates.

High MB response fraction (ie high density, or low sparsity) correlated strongly with high SNR (ie reliability of intra-class EN responses). But it also resulted in poor post-training classifier accuracy, because Hebbian growth was not focused: Rather, it boosted all weights due to the excess of active MB neurons, so weight increases into a particular EN were not restricted to just the most class-relevant MB signals. The EN then responded strongly to all digits rather than just its target digit.

Conversely, low MB response (ie high sparsity) resulted in low intra-class SNR, since not enough MB neurons would fire in response to a digit for reliable activation of the ENs. But high sparsity correlated strongly with high “learning focus”: Training focused gains on the correct class, ensuring that ENs’ responses to their targeted digits were preferentially strengthened. This resulted in stronger post-training accuracy.

Post-training discrimination accuracy appeared to represent an optimized trade off between intra-class SNR and learning focus. The tradeoff is shown in Fig 4.5, which plots these effects of different sparsity levels in the MB, as they relate to learning:

Descending red curve. This plots “learning focus”, a figure-of-merit defined as the average standardized distance between EN response distributions to trained and control classes,

$$(4.1) \quad LF = \frac{1}{9} \sum_{i \neq j} \frac{(\mu E_{jj} - \mu E_{ji})}{0.5(\sigma E_{jj} + \sigma E_{ji})}, \text{ notation as in Eqn 3.1.}$$

This is average Bhattacharyya distance if EN response distributions are gaussian. In very sparse regimes training was strongly focused on the trained class, while in dense regimes training “raised all boats” and the trained response distributions were very poorly separated. Thus high sparsity focused learning well, and low sparsity diluted it.

Ascending black dotted curve. This plots the mean intra-class signal-to-noise ratio (SNR):

$$(4.2) \quad \text{SNR} = \frac{\mu(f)}{\sigma(f)} \text{ where } f = \text{EN odor response};$$

This was an opposite situation: A very sparse MB resulted in high intra-class variance in trained EN responses (low SNR), while a denser MB delivered much more consistent within-class responses (high SNR).

Domed blue curve. This is a fit to classifier accuracies from experiment. Post-training accuracy is a natural objective function.

Judged by best post-training classification accuracy, optimal MB sparsity level for MothNet appears to represent a compromise between delivering sufficient intra-class SNR and sufficient “learning focus” for inter-class distinctions. This optimal region lies somewhere between 5-20%, consistent with the 5-15% commonly observed in live BNNs.

5. Discussion.

A biological toolkit for building NNs.

Our goal has been to provide a proof-of-concept as to the learning abilities of even the simplest of biological neural networks (BNNs), and to clarify how a NN built from biological elements learns a predictive model for a general ML task.

In order to learn new odors, the moth olfactory network uses just a few core tools: A noisy pre-amp network with competitive inhibition; Hebbian plasticity controlled by a high-dimensional sparse layer; and generalized (global) stimulation during training.

Our key finding is that a neural net built with this biological toolkit can succeed at a general rapid-learning task, and in fact can out-perform standard ML methods. MothNet learned to read MNIST digits, increasing its accuracy more than 5x (from 15% to 75-85%) given only a few training samples (1-20 per class). Also, because Hebbian weight updates focus entirely on activity induced by the class being trained (not on activity induced by control classes, as in backprop), new classes can be added and trained without retraining on existing classes.

This finding is of interest because the biological tools analyzed here are well-suited to being combined and stacked into larger, deeper neural nets, just as convolutional kernels, maxpool, etc, are combined to build current DNNs. The success of live BNNs at a wide range of tasks argues for the potential of NNs built with a biological toolkit to succeed at ML tasks.

We note that in these experiments MothNet stayed close to the moth’s very simple olfactory architecture, and used a simple feature set as input (pixels). We believe that a free hand with network design, such as using better input features, biologically-unrealistic model parameters, and more complex architectures, would yield stronger results in a variety of tasks. This effect has been demonstrated by biological brains of increased size and complexity, and

indeed by increasingly complex DNNs.

The rapid learning regime.

It is not, on reflection, surprising that an insect brain might out-perform ML methods at a few-samples learning task. First, BNNs in general excel at rapid learning from few samples. Second, in the typical ML context, such as a competition or a comparison with other methods using well-defined benchmarks, the number of training samples is fixed and is often high (eg 60,000 for MNIST). The competitive pressure is to maximize accuracy, with no penalty for using lots of training data. In sharp contrast, an insect pays a high cost for every extra training datum, and their competitive pressure is to very rapidly attain “good-enough” accuracy.

These two regimes complement each other, and there are applications where it may be advantageous to pair a fast, rough learner with a slower, more precise learner. One example might be an adaptive controls learner for a drone: If the drone collides in mid-air and loses an engine, you eventually want to learn a new, optimal control strategy for the reduced system. But the first necessity is to learn a “good enough” control strategy very fast, before crashing, to allow time for the subtler system to train. Another example might be a multi-stage bootstrap labeling scheme when labeled data are scarce: In the initial stage, given just one or a few labeled samples, the fast learner might classify and apply labels to more samples (perhaps keeping only those with the most certain labels) until there are enough labeled samples to train a subtler system as the second stage labeler.

Role of the sparse layer.

A second finding emphasizes the key role of sparse layers during learning. Sparse, high-dimensional layers are a widespread motif in biological neural systems, especially in networks related to memory and plasticity [32]. In the moth, the sparse layer (MB) plays a vital role in learning because all the plastic synapses connect into or out of the sparse layer, allowing it to modulate the Hebbian updates to the synaptic connections by taking advantage of the fact that Hebbian growth is an AND gate (“fire-together, wire-together”). This ensures that learning boosts the important signal (ie the signal associated with a given sample) and not artifacts.

While the sparse MB layer calls to mind the backprop sparse autoencoder [33], the biological role described here has no obvious analogue in backprop sparse encoders, since it is tied to the Hebbian update method. However, biological sparse layers may also perform functions similar to those found in backprop sparse autoencoders, such as reducing noise [34] and reducing the dimension of the feature space in order to better match the essential dimension of the classification task [35].

Role of octopamine.

Unanswered by these experiments is whether generalized stimulation by octopamine is required in ML systems such as MothNet, distinct from actual biological systems. In the moth, octopamine stimulation may offer a work-around to avoid biological constraints on Hebbian growth rates and input intensity. That is, octopamine may act primarily as an accelerant. However, engineered NNs can easily crank up growth rates, enforce higher MB activity, and amplify signals during training, all without recourse to the octopamine mechanism but per-

haps with the same beneficial effect on learning. In this case, generalized stimulation would not be a necessary part of the biological toolkit described here for application to ML tasks. However, it may be that octopamine stimulation also enables exploration of the coding solution space not normally activated by stimuli. Alternate ways to replace this functionality in the ML context are not so obvious.

Role of noise.

Also unexplained is the role, if any, of high intrinsic noise in the Antennal Lobe during learning. The fact that noise carries no penalty to learning would partly explain its existence in any biological system which found noise desirable for other reasons. However, our experiments found no positive reason to build high intrinsic noise into the AL (or any NN layer) in an ML context. However, a noisy pre-amp (eg the AL) might still be actively beneficial, despite our results, for three reasons.

First, when coupled with sniffing, a noisy AL might provide a version of data augmentation (as used in DNNs) by distorting the codes delivered to the MB and readout neurons. This would improve one-shot or few-shot learning, if the distortions induced by the noisy AL somewhat mimicked the within-class sample variation (this condition was likely absent in our MNIST experiments). Second, injecting noise into input layers, or corrupting training samples, can improve NN classification performance [36], suggesting a concrete benefit during training (though perhaps not during classification). Third, injecting noise may be a useful or even necessary way to explore the solution space [37].

Expanding the biological toolkit.

The set of algorithmic tools for learning characterized here derive from one of the simplest biological learning networks (a bug brain). It is still unclear whether modifications to this network can substantially improve performance, or whether this particular architecture can achieve just so much in terms of accuracy and scope of work, commensurate with the constrained needs and pressures experienced by insects as they evolved. Happily, BNNs are incredibly diverse and complex. So countless other useful elements can likely be abstracted from other biological systems and applied to ML tasks. This requires accurately modeling these more complex systems and analyzing how they learn, an open-ended task.

Computer code for this paper will be found at:

<https://github.com/charlesDelahunt/PuttingABugInML>

REFERENCES

- [1] Fukushima K. Neocognitron: A Self-Organizing Neural Network Model for a Mechanism of Pattern Recognition Unaffected by Shift in Position. *Biological Cybernetics*. 1980;36:193–202.
- [2] Hubel D, Wiesel T. Receptive fields, binocular interaction, and functional architecture in the cat's visual cortex. *Journal of Physiology*. 1962;160:106–154.
- [3] Schmidhuber J. Deep learning in neural networks: An overview. *Neural Networks*. 2015;61(Supplement C):85 – 117. Available from: <http://www.sciencedirect.com/science/article/pii/S0893608014002135>.
- [4] Goodfellow I, Bengio Y, Courville A, Bengio Y. Deep learning. vol. 1. MIT press Cambridge; 2016.
- [5] LeCun Y, Bengio Y, Hinton G. Deep learning. *Nature*. 2015;521(7553):436.
- [6] Riffell JA, Lei H, Abrell L, Hildebrand JG. Neural Basis of a Pollinator's Buffet: Olfactory Specialization and Learning in *Manduca sexta*. *Science*. 2012;Available from: <http://science.sciencemag.org/content/early/2012/12/05/science.1225483>.
- [7] Galizia CG. Olfactory coding in the insect brain: data and conjectures. *European Journal of Neuroscience*. 2014;39(11):1784–1795. Available from: <http://dx.doi.org/10.1111/ejn.12558>.
- [8] Caron S, Ruta V, Abbott L, Axel R. Random convergence of olfactory inputs in the *Drosophila* mushroom body. *Nature*. 2013;497(5):113–7.
- [9] Cassenaer S, Laurent G. Hebbian STDP in mushroom bodies facilitates the synchronous flow of olfactory information in locusts. *Nature*. 2007 Jun;448:709 EP –. Available from: <http://dx.doi.org/10.1038/nature05973>.
- [10] Masse NY, Turner GC, Jefferis GSXE. Olfactory Information Processing in *Drosophila*. *Current Biology*. 2009;19(16):R700 – R713. Available from: <http://www.sciencedirect.com/science/article/pii/S0960982209013013>.
- [11] Campbell RAA, Turner GC. The mushroom body. *Current Biology*. 2010;20(1):R11 – R12. Available from: <http://www.sciencedirect.com/science/article/pii/S096098220901851X>.
- [12] Honegger KS, Campbell RAA, Turner GC. Cellular-Resolution Population Imaging Reveals Robust Sparse Coding in the *Drosophila* Mushroom Body. *Journal of Neuroscience*. 2011;31(33):11772–11785. Available from: <http://www.jneurosci.org/content/31/33/11772>.
- [13] Babadi B, Sompolinsky H. Sparseness and Expansion in Sensory Representations. *Neuron*. 2014;83(5):1213 – 1226. Available from: <http://www.sciencedirect.com/science/article/pii/S0896627314006461>.
- [14] Hammer M, Menzel R. Learning and memory in the honeybee. *Journal of Neuroscience*. 1995;15(3):1617–1630. Available from: <http://www.jneurosci.org/content/15/3/1617>.
- [15] Hammer M, Menzel R. Multiple Sites of Associative Odor Learning as Revealed by Local Brain Microinjections of Octopamine in Honeybees. *Learn Mem*. 1998 May;5(1):146–156. 10454379[pmid]. Available from: <http://www.ncbi.nlm.nih.gov/pmc/articles/PMC311245/>.
- [16] Wilson RI. Neural and behavioral mechanisms of olfactory perception. *Current Opinion in Neurobiology*. 2008;18(4):408 – 412. Sensory systems. Available from: <http://www.sciencedirect.com/science/article/pii/S0959438808000883>.
- [17] Dacks A, Riffell J, Martin J, Gage S, Nighorn A. Olfactory modulation by dopamine in the context of aversive learning. *Journal of Neurophysiology*. 2012 7;108(2):539–550.
- [18] Delahunt CB, Riffell JA, Kutz JN. Biological Mechanisms for Learning: A Computational Model of Olfactory Learning in the *Manduca sexta* Moth, with Applications to Neural Nets. *arXiv*. 2018;Available from: <https://arxiv.org/abs/1802.02678>.
- [19] LeCun Y, Cortes C. MNIST handwritten digit database. Website. 2010;Available from: <http://yann.lecun.com/exdb/mnist/> [cited 2016-01-14 14:24:11].
- [20] Martin JP, Beyerlein A, Dacks AM, Reisenman CE, Riffell JA, Lei H, et al. The neurobiology of insect olfaction: Sensory processing in a comparative context. *Progress in Neurobiology*. 2011;95(3):427 – 447. Available from: <http://www.sciencedirect.com/science/article/pii/S0301008211001742>.
- [21] Kvello P, Lfaldli B, Rybak J, Menzel R, Mustaparta H. Digital, three-dimensional average shaped atlas of the *Heliothis virescens* brain with integrated gustatory and olfactory neurons. *Frontiers in Systems Neuroscience*. 2009;3:14. Available from: <https://www.frontiersin.org/article/10.3389/neuro.06.014.2009>.

[22] Bhandawat V, Olsen SR, Gouwens NW, Schlief ML, Wilson RI. Sensory processing in the Drosophila antennal lobe increases reliability and separability of ensemble odor representations. *Nature Neuroscience*. 2007;10:1474–1482.

[23] Perisse E, Burke C, Huettner W, Waddell S. Shocking Revelations and Saccharin Sweetness in the Study of Drosophila Olfactory Memory. *Curr Biol*. 2013 Sep;23(17):R752–R763. S0960-9822(13)00921-4[PII], 24028959[pmid]. Available from: <http://www.ncbi.nlm.nih.gov/pmc/articles/PMC3770896/>.

[24] Bazhenov M, Stopfer M. Forward and Back: Motifs of Inhibition in Olfactory Processing. *Neuron*. 2010;67(3):357 – 358. Available from: <http://www.sciencedirect.com/science/article/pii/S0896627310005842>.

[25] Campbell R, Honegger K, Qin H, Li W, Demir E, Turner G. Imaging a Population Code for Odor Identity in the Drosophila Mushroom Body. *Journal of Neuroscience*. 2013;33(25):10568–81.

[26] Hige T, Aso Y, Rubin GM, Turner GC. Plasticity-driven individualization of olfactory coding in mushroom body output neurons. *Nature*. 2015 Sep;526:258 EP –. Available from: <http://dx.doi.org/10.1038/nature15396>.

[27] Dayan P, Abbott LF. Theoretical Neuroscience: Computational and Mathematical Modeling of Neural Systems. The MIT Press; 2005.

[28] Higham DJ. An Algorithmic Introduction to Numerical Simulation of Stochastic Differential Equations. *SIAM Rev*. 2001 Mar;43(3):525–546. Available from: <http://dx.doi.org/10.1137/S0036144500378302>.

[29] Hebb DO. The organization of behavior : a neuropsychological theory. Wiley New York; 1949.

[30] Murphy KP. Machine Learning: A Probabilistic Perspective. The MIT Press; 2012.

[31] LeCun Y, Jackel L, Bottou L, Brunot A, Cortes C, Denker J, et al. Comparison of Learning Algorithms for Handwritten Digit Recognition. In: International Conference on Artificial Neural Networks; 1995. p. 53–60.

[32] Ganguli S, Sompolinsky H. Compressed Sensing, Sparsity, and Dimensionality in Neuronal Information Processing and Data Analysis. *Annual Review of Neuroscience*. 2012;35(1):485–508. PMID: 22483042. Available from: <https://doi.org/10.1146/annurev-neuro-062111-150410>.

[33] Ng A. Sparse Autoencoder. Webpage. 2010; Available from: <https://web.stanford.edu/class/archive/cs/cs294a/cs294a.1104/sparseAutoencoder.pdf>.

[34] Vincent P, Larochelle H, Bengio Y, Manzagol PA. Extracting and Composing Robust Features with Denoising Autoencoders. In: Proceedings of the 25th International Conference on Machine Learning. ICML '08. New York, NY, USA: ACM; 2008. p. 1096–1103. Available from: <http://doi.acm.org/10.1145/1390156.1390294>.

[35] Makhzani A, Frey BJ. k-Sparse Autoencoders. *CoRR*. 2013;abs/1312.5663. Available from: <http://arxiv.org/abs/1312.5663>.

[36] An G. The Effects of Adding Noise During Backpropagation Training on a Generalization Performance. *Neural Comput*. 1996 Apr;8(3):643–674. Available from: <http://dx.doi.org/10.1162/neco.1996.8.3.643>.

[37] Bengio Y, Fischer A. Early Inference in Energy-Based Models Approximates Back-Propagation. *arXiv e-prints*. 2015 Oct;abs/1510.02777. Available from: <https://arxiv.org/abs/1510.02777>.